DNA Nanostructure

DOI: 10.1002/anie.201402973

Helical DNA Origami Tubular Structures with Various Sizes and Arrangements**

Masayuki Endo, Seigi Yamamoto, Tomoko Emura, Kumi Hidaka, Nobuhiro Morone, John E. Heuser, and Hiroshi Sugiyama**

Abstract: *We developed a novel method to design various helical tubular structures using the DNA origami method. The size-controlled tubular structures which have 192, 256, and 320 base pairs for one turn of the tube were designed and prepared. We observed the formation of the expected short tubes and unexpected long ones. Detailed analyses of the surface patterns of the tubes showed that the short tubes had mainly a left-handed helical structure. The long tubes mainly formed a right-handed helical structure and extended to the directions of the double helical axes as structural isomers of the short tubes. The folding pathways of the tubes were estimated by analyzing the proportions of short and long tubes obtained at different annealing conditions. Depending on the number of base pairs involved in one turn of the tube, the population of left-/right-handed and short/long tubes changed. The bending stress caused by the stiffness of the bundled double helices and the non-natural helical pitch determine the structural variety of the tubes.*

The programmed assembly of DNA molecules has been widely used for the design of various nanostructures[1–5] and the creation of precisely designed nanoscale functional materials.[6–8] DNA tubular structures, the most essential 3D nanostructure, were initially developed by simply connecting both edges of DNA tiles along the helical axes.[9–12] Subsequently, the geometry of neighboring helices in the bundled double-stranded DNAs (dsDNA) was precisely designed to fold into defined tubular structures.[13–15] In the DNA origami design, six-helix-bundled tubes were first created for the construction of 3D architectures,[2,16] then twisted bundled tubes were developed by changing the helical pitches in the bundled dsDNAs.[17] Recently, spherical shapes and objects were created by adjusting the crossover positions and helical pitches.[18]

Herein, we created a new type of tubular structures differing from conventional DNA tubes. Those new DNA tubes with various diameters and lengths were designed by connecting a winding tape to form a helical assembly. We designed tubular structures by considering the folding of long tape structures consisting of an antiparallel double dsDNA bundle (Figure 1). In this design, the number of base pairs involved in one turn of the tube and the numbers of layers can be defined. We designed three tubular structures termed 6-, 8-, and 10-tube, which contained 192, 256, and 320 base pairs (bp) in one turn of the tube, respectively. The direction of the double helices should affect the left-handed and right-handed helical structures; however, we cannot predict the helical

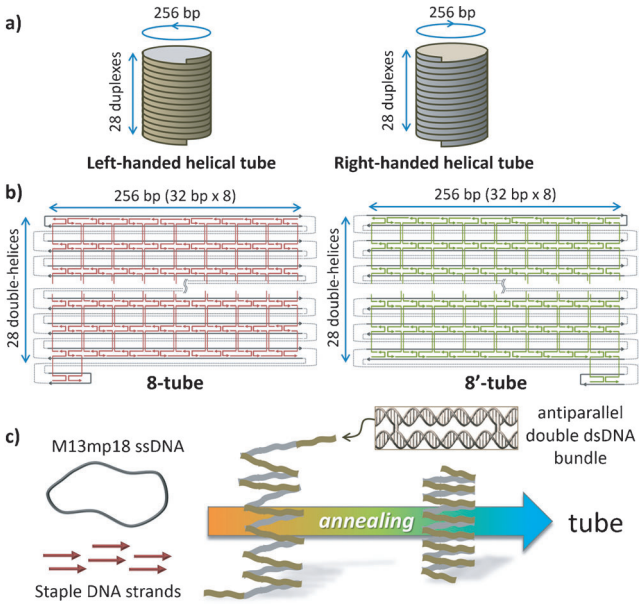

Figure 1. Designs of the helical tubular structures. a) Two chiralities of helical tubes, left-handed and right-handed ones, which could be formed. b) Designs of the 8- and 8′-tube. In these designs, the 28 layers of 256 bp of dsDNA are helically assembled to form a tubular structure. The double dsDNA bundle of the 8- and 8′-tube start from left top and right top, respectively. Black and colored lines represent M13mp18 ssDNA and staple DNA strands, respectively. c) A conceptual scheme for the tube formation from M13mp18 ssDNA and staple DNA strands. By decreasing the temperature, the tape-like antiparallel double dsDNA bundle assembles side-by-side to finally form a tubular structure.

[*] Prof. Dr. M. Endo, K. Hidaka, Dr. N. Morone, Prof. Dr. J. E. Heuser, Prof. Dr. H. Sugiyama
Institute for Integrated Cell-Material Sciences (WPI-iCeMS)
Kyoto University
Yoshida-ushinomiyacho, Sakyo-ku, Kyoto 606-8501 (Japan)
E-mail: endo@kuchem.kyoto-u.ac.jp
hs@kuchem.kyoto-u.ac.jp
S. Yamamoto, T. Emura, Prof. Dr. H. Sugiyama
Department of Chemistry, Graduate School of Science
Kyoto University
Kitashirakawa-oiwakecho, Sakyo-ku, Kyoto 606-8502 (Japan)

[**] This work was supported by Core Research for Evolutional Science and Technology (CREST) of JST and JSPS KAKENHI (grant no. 24310097, 24104002) to M.E., (grant no. 24225005) to H.S., (grant no. 25253004) to J.E.H., and (grant no. 23310087) to N.M. Financial support from The Mitsubishi Foundation and The Asahi Glass Foundation to M.E. are also acknowledged.

Supporting information for this article is available on the WWW under http://dx.doi.org/10.1002/anie.201402973.

properties of the tubes before assembling them. Therefore, we examined the helical directions of the assembled tubes by studying their surfaces with atomic force microscopy (AFM). The tube surface should present a bundled dsDNA pattern in which multiple dsDNAs are connected by crossovers.

We first designed a tubular structure with 256 bp in one turn of the tube and 28 layered bundled double helices as the tube body (Figure 1a). This structure was named 8-tube, because it had eight crossover points in one turn. Two origami designs, 8-tube and 8′-tube, were prepared, in which the double dsDNA bundle started from the left top side and the right top side, respectively (Figure 1b). These assemblies should have preferential chirality according to the different directional design of double dsDNA bundles in the 8- and 8′-tube, which are expected to form two different tubular structures, left-handed and right-handed helical tubes.

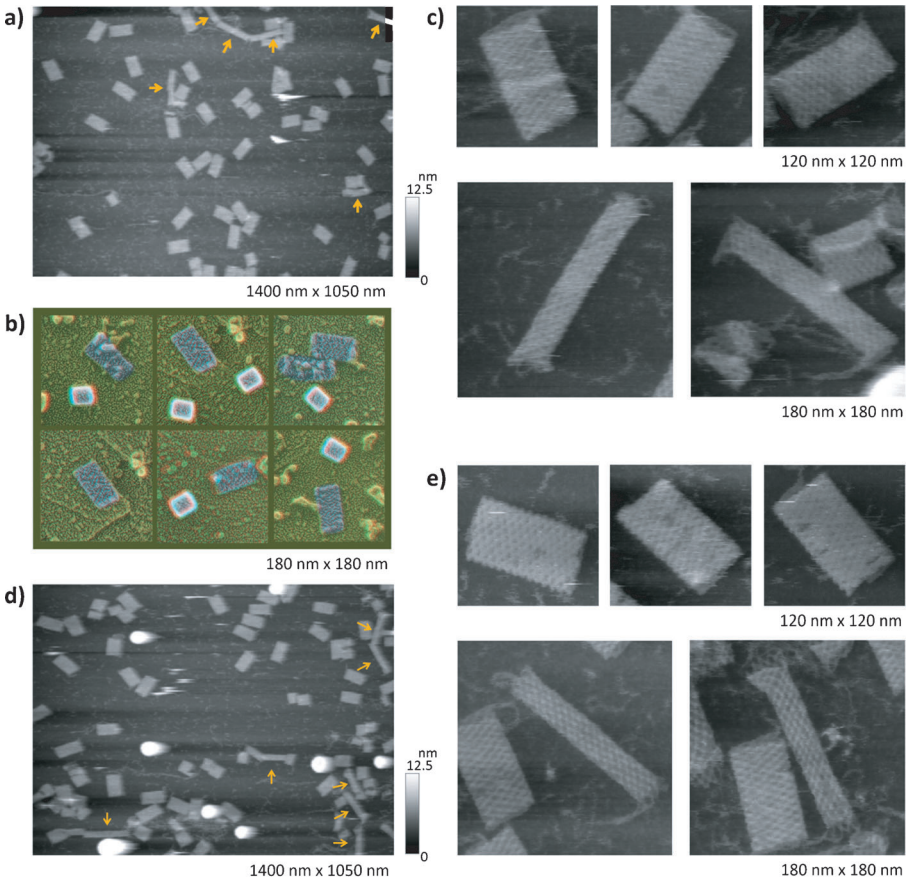

Figure 2. AFM images of helical tubes and their detailed surface patterns. a) AFM image of the 8-tubes after assembly. The orange arrows represent long tubular structures. b) Electron microscope images of short 8-tubes obtained using the quick-freeze/mica flake technique. The smaller cylinder in the images is hemocyanin (right-handed helical structure). c) Detailed AFM images of individual short and long 8-tubes. d) AFM image of the 8′-tubes after assembly. The orange arrows represent long tubular structures. e) Detailed AFM images of individual short and long 8′-tubes.

First, we prepared the sample using 10 nM M13mp18 ssDNA (7249 nucleotides, nt), 50 nM staple DNA strands (5 equiv), 20 mM Tris buffer (pH 7.6), 10 mM $MgCl_2$, and 1 mM EDTA. The tubular structure was assembled by annealing from 85 °C to 15 °C at a rate of −0.5 °C min^{-1}. The assembled structures were directly investigated by AFM. In the AFM images scanned at 0.1 frame s^{-1}, the tubular structures were mobile on the mica surface during the scanning process, possibly because of the stiffness of the tube surface. (Figure S1). Therefore, we treated a mica with 3-aminopropyl trimethoxysilane (APTES) to achieve a tight attachment of the DNA tubes on the cationic surface. After the tube assembly, we observed clear periodic patterns on the surface of the tube body (Figure 2). The surface pattern of the tube body was similar to that of planar DNA origami nanostructures.[19] In addition, we found two different shapes of tubes in the AFM images of 8-tube (Figures 2a,c and S2) and 8′-tube (Figures 2d,e and S3): the expected short ones and unexpected long ones. The tubular structures were also investigated by electron microscopy (Figures 2b and S4).[20] A periodic pattern was also observed on the surface and inside the tube after the structures were fractured (Figure S4).

Cross-sectional analyses of tubes in the AFM images revealed that the observed tubes were crushed two-layered structures whose heights were twice larger than that of a usual dsDNA (1.5–2.0 nm) (Figures S2 and S3). These structures are often observed on the mica for hollow structures such as tubular and prism structures.[4,9] The short tubes were always found to be higher than the long tubes, probably because of the stiffness of the bundled double helices in the tube body. The observed length and width of the tubes are summarized in Table 1. Both short tubes had a length of 92–95 nm and consisted of 28 layers of bundled dsDNAs, so that the width of one layer of dsDNA was calculated to be 3.3–3.4 nm. The diameter of the tubes was estimated from their width to be 29–30 nm. These values were close to the expected diameter (28 nm) of the designs when it is roughly calculated based on the circumference of 256 bp (87 nm).

Table 1: Measurement of the dimensions (in nm) of 8- and 8′-tube.[a]

	8-tube short	8-tube long	8′-tube short	8′-tube long
length	92.1 ± 3.6	162.1 ± 5.4	94.9 ± 3.6	160.7 ± 8.3
width	46.1 ± 2.2	24.1 ± 1.5	47.7 ± 2.2	22.2 ± 2.5

[a] Mean values ± standard deviation.

We next analyzed the surface patterns of both tubular structures in detail (Figure 3). The surface pattern of the tubes was similar to a planar origami tile.[19] In the short tubes, the

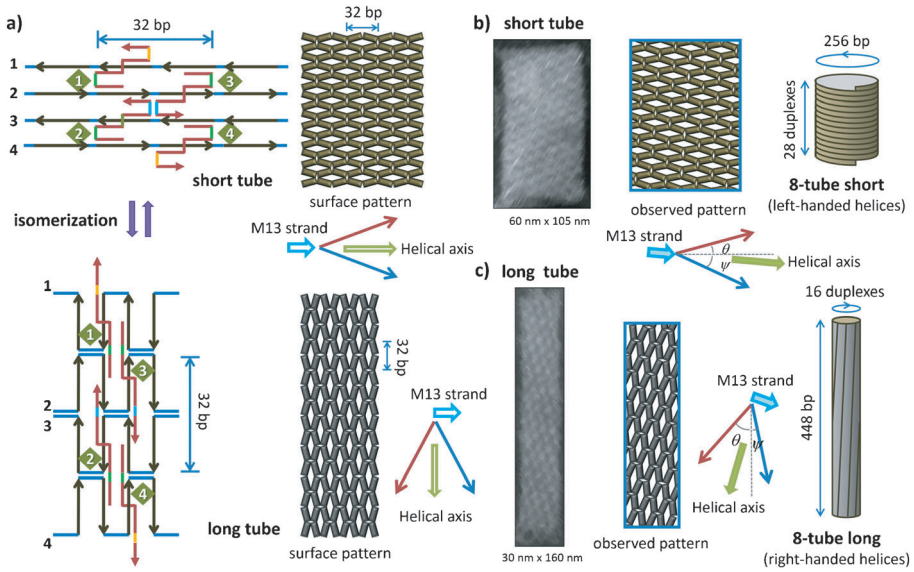

Figure 3. Two different tubular structures observed after assembly. Analyses of their arrangements and surface patterns. a) Two possible arrangements for tubular assemblies. The dark gray and red lines represent the M13 strand and staple DNA strands, respectively. The crossover points are indicated by blue lines and the numbers represent the M13 strand and staple strands. The expected surface patterns for both arrangements are shown. The blue and red arrows represent the directions of the observed patterns, and the open light blue and green arrows represent the direction of M13 strand and that of the bundled dsDNA axes (helical axis), respectively. b) AFM image and illustration of the surface pattern of a short helical tube and the angles used for measurement (θ and ψ). c) AFM image and illustration of the surface pattern of a long helical tube, and the angles used for measurement (θ and ψ). The estimated long 8-tube structure with right-handed helices is shown on the right.

surface pattern originated from the double helices and crossovers and was analyzed by measurement of the angles of the observed surface pattern. When the bundled dsDNAs in the DNA origami structure were curved in one direction, left-handed or right-handed tubes should be formed depending on the helical stress caused by the underwound twists between the adjacent crossovers (Figure 1). The two angles, θ and ψ, from the horizontal direction of the short tube showed that the direction of the helical axes slightly declined downward (Figure 3b and Table 2). This measurement showed that the left-handed helical tube was a major product. In the case of the short 8-tube, left-handed tubes were formed in ca. 85% yield. In the case of the 8′-tube, the proportions of short/long and right-handed/left-handed tube were similar to those of the 8-tube.

Next, we analyzed the long-tube structures in detail and estimated the connection pattern in the long tubes (Figure 3). Interestingly, the surface pattern of the long tubes exhibited a different arrangement of bundled dsDNAs compared with that of the short tubes (Figure 3b). Based on this surface pattern, the helical axes of bundled dsDNAs were extended into the direction parallel to the axis of the long tube with a twist. In the initial design of the short tube, the axes of bundled dsDNAs should run around the tube, meaning that the direction of the helix should be perpendicular to the axis of the tube. In the observed pattern of the long tube, the M13 ssDNA formed multiple turns at crossover points, whereas the staple strands formed a usual helix without turns (Figure 3a left bottom). This finding shows that the short and long tubes are isomeric tubular structures, in which the directions of helical axes are completely different (Figure 3a).

As seen in the Holliday junction, two adjacent dsDNAs can change their relative positioning and conformation at the crossover point, and the conformations can be switched by imposing the force outside.[21,22] In the planar DNA origami structure, the M13 ssDNA strand runs in a linear fashion, and the staple DNAs fold back at crossover points.[19] In the case of the helical tubular structure, the curved tube surface imposes structural stress to the bundled dsDNAs along the axial direction, which induces structural isomerization at crossover points to stabilize the isomer (Figure 3a). In this arrangement, staple DNAs form double helices with a kinked M13 ssDNA, which arranges in a zigzag form. In Figure 3b,c the directions along the M13 ssDNA chain in the short and long tubes are both left-handed helices. This means that the short and long tubes shown here are just structural isomers of the same structure. We concluded that the long tubes were the vertically expanded isomeric structure of the corresponding short tubes.

Table 2: Observed angles (in °) on the tube surface of short and long 8- and 8′-tubes.[a,b]

	8-tube short		8-tube long		8′-tube short		8′-tube long	
Direction of M13 strand	L	R	L	R	L	R	L	R
Direction of helical axes	L	R	R	L	L	R	R	L
angle θ	28.6 ±1.9	34.4 ±2.0	41.6 ±4.0	18.1 ±1.2	28.2 ±1.6	32.8 ±2.4	39.8 ±3.1	17.5 ±2.7
angle ψ	31.9 ±1.7	27.9 ±1.6	15.9 ±3.1	41.4 ±2.1	33.5 ±1.9	30.8 ±1.1	14.8 ±2.5	40.8 ±3.4
tubes analyzed	29	5	25	1[c]	26	6	24	7

[a] Mean values ± standard deviation. [b] L: left-handed, R: right-handed. [c] Three different positions of the tube were measured.

The measurement of the two angles θ and ψ from the direction parallel to the long tube axis showed that the

direction of the helices largely declined downward (Figure 3c). The length of the long tubes, which consisted of 448 bp of bundled dsDNAs, was ca. 160 nm. This value is close to the expected length (152 nm). The width of long tubes, which consisted of 16 bundled dsDNAs, was 44–48 nm, and the center-to-center distance between two neighboring dsDNAs was calculated to be 2.8–3.0 nm. Therefore, the diameter of the long tubes was estimated to be 14–15 nm.

In the long-tube structure, both ends of the tube were termini of the helical axes of 16 bundled dsDNAs. In the AFM images, the short tubes were monodisperse, while the long tubes were often connected at their termini (Figure 2a,d). This also indicates that the termini of long tubes have adhesive ends for π-stacking interactions, as observed in the DNA origami structures.[19]

To estimate the folding process of tubular structures, we next examined the formation of the short and long tubular structures by changing the annealing conditions (Figure 4). Three different annealing speeds, $-0.1\,^{\circ}C\,min^{-1}$ (slow), $-0.5\,^{\circ}C\,min^{-1}$ (usual), and $-2.0\,^{\circ}C\,min^{-1}$ (fast) were examined. The tubular structures were assembled using these conditions and confirmed by AFM. Under the slow annealing conditions, the formation of long tubes was suppressed (6% yield), and the short-tube formation was dominant (Figure 4a). By using the fast annealing conditions, the proportion of long tubes increased dramatically (28% yield). Figure 4b shows the gel image of the short/long-tube formation using the three different annealing conditions. Slow annealing gave almost a single band corresponding to short tubes, which was confirmed by recovering the short tubes from the band, whereas a smeared band corresponding to long tubes was observed in the fast and usual annealing conditions. These results show that the annealing speed is critical for the formation of the short and long tubes.

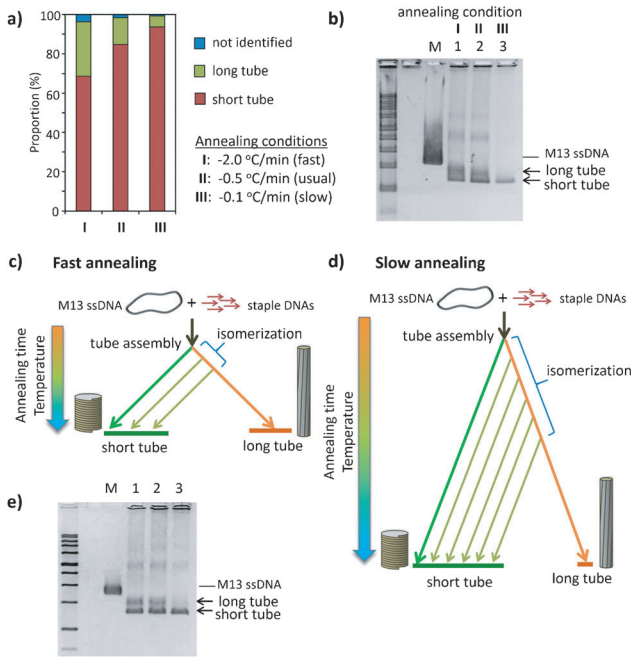

Figure 4. The folding process of helical tubular structures. a) Proportion of the formation of the short and long 8-tube using different annealing conditions. Morphology of the tubes was analyzed using the AFM images. b) Gel electrophoresis image of the short/long tube formation. c,d) Proposed self-assembly process into two different tubes depending on the annealing speed. e) Gel electrophoresis image of the short/long tube formation using fast annealing (lane 1) followed by slow reannealing from 37°C (lane 2) and 50°C (lane 3).

We estimated the relationship between the annealing conditions and short/long-tube formation. Because long tubes require large numbers of hairpin turns of the M13 strand for correct folding (Figure 3a), the formation of long tubes should be structurally unfavorable compared with the simple short tube. We proposed the formation of short and long tubes (Figure 4c,d). At the initial assembly, there was no preference for folding into a left- or right-handed coil. In the initial hybridization at higher temperature, both left- and right-handed arrangements were possible. By decreasing the temperature, the tubes were folded in structurally favorable arrangements to reduce the structural stress. During the initial folding of a tubular structure, pre-right-handed tubes were rearranged to become less structurally stressed left-handed tube. Subsequently, less stable long tubes were isomerized to form short tubes during annealing, resulting in the formation of the left-handed short tube as a major product. Therefore, in the case of fast annealing conditions, there was not sufficient time for the isomerization from a long to a short tube, so that the long tubes were left unchanged during rapid cooling. This explanation was further supported by reannealing from a lower temperature to control the short/long-tube proportion. The tubes were prepared by fast annealing, followed by the slow annealing from 37 or 50°C. Figure 4e shows the gel image of the short/long-tube formation using this annealing procedure. In the case of reannealing from 50°C, the short-tube formation increased (lane 3) compared with that using the fast annealing process (lane 1), whereas no change in the short/long-tube proportion was observed by reannealing from 37°C (lane 2). These results indicate that the isomerization from long to short tubes seems to occur at around 50°C and that the short tube formation is thermodynamically favored, while the long tube should be a kinetically trapped form.

We also examined the isothermal assembly of the 8-tube using heating denaturation (65°C, 15 min) followed by decreasing the temperature to a value between 40 to 60°C (2°C intervals, 2 h; Figures S5 and S6).[23] When assembled at 56°C, the tubular structures were found to be formed as well as when using the usual annealing conditions. Incomplete tubes increased by lowering the isothermal temperature. We also investigated the isomerization temperatures using fast annealing followed by assembly at a constant temperature (36–56°C) (Figures S7 and S8). Using this method, we found many incompletely isomerized tubes in the AFM images; the centers of these tubes were narrower and both ends were wider. Although we could not determine the clear threshold temperature for the isomerization, these isothermal method also worked for the tube assembly and isomerization.

In the present design, the left-handed helical short tube was a major product over the right-handed one. To control the formation of left-handed and right-handed helical tubes, we adjusted the number of base pairs between crossovers. In the DNA origami design, the average helical pitch is 10.67 bp/

turn (32 bp for 3-turns),[19] which is slightly underwound from 10.5 bp/turn of a native dsDNA pitch. This causes global twisting of the planar structure that consists of bundled dsDNAs.[24] Thus, we assumed that overwound helices would make a twist for producing a right-handed short tube structure in contrast to underwound helices. We used designs for the construction of right-handed short tubes with a 10.33 bp/turn pitch (31 bp per 3-turns), which is an overwound helix compared with the usual 10.5 bp/turn pitch. The designed structures were assembled using the usual annealing conditions. The AFM images (Figure S9) revealed that right-handed short tubes increased to be ca. 45% by changing the helical pitch from 10.67 bp/turn to 10.33 bp/turn (ca. 15% using the 10.67 bp/turn pitch). This result indicates that the overwound helices generate a torque that can change the twist of bundled dsDNAs during the tube formation, and the helical pitch is the main factor to determine the global change of the helical direction of the tubes.

To expand the design of the helical tubular structures, we prepared tubes with two different diameter sizes: 6-tubes with 38 layers of dsDNA and 192 bp per turn (Figure 5a), and 10-tubes with 22 layers of dsDNA and 320 bp per turn (Figure 5e). The gel electrophoresis of these tubes using various annealing conditions is shown in Figure S10. The observed lengths and widths of 6- and 10-tubes are summarized in Table 3. The observed angles of surface patterns of 6- and 10-tubes are summarized in Table 4.

In the 6-tube, the tubular structure was assembled by annealing from 85 °C to 15 °C at a rate of $-0.5\,^{\circ}\mathrm{C\,min^{-1}}$. Short and long tubes were observed in AFM images, and the proportion of the short and long 6-tubes was 41% and 45%, respectively (Figures 5b,i and S11). Using the fast annealing conditions, the long 6-tubes (68% yield) formed almost four times more efficiently than the short 6-tubes (16% yield) (Figure 5i). These results indicate that the expected short 6-tube is structurally not favorable compared with the long 6-tube. The detailed analyses of the surface of short and long tubes showed that left-handed helical structures were the main species for short tubes (ca. 85%), and that long tubes exhibited mainly right-handed helices (ca. 85%). The length of short 6-tubes, which consisted of 38 layers of bundled dsDNAs, was 119 nm, so that the width of one layer was calculated to be 3.1 nm. The diameter of short 6-tubes was estimated to be 21 nm from the width of the tube. This value was close to the diameter expected from the design (21 nm), when the diameter was roughly calculated from the circumference of 192 bp (65 nm). The length of long 6-tubes consisting of 608 bp of bundled dsDNAs, was 202 nm. This value was also close to the expected length (207 nm). The width of long 6-tubes, which consisted of 12 bundled dsDNAs, was 14 nm, and the center-to-center distance between adjacent helices was calculated to be 2.3 nm. Therefore, the diameter of long 6-tubes was estimated to be 9 nm. To assemble the short 6-tubes, the involved bundled dsDNAs need to be largely curved. This imposes a structurally strong stress on the bundled dsDNA axes. Therefore, the short tube should not be structurally favorable. Conversely, the long tube with 12-helix-bundled dsDNAs may be relatively stable compared with the short tube. We also observed the long/short mixed

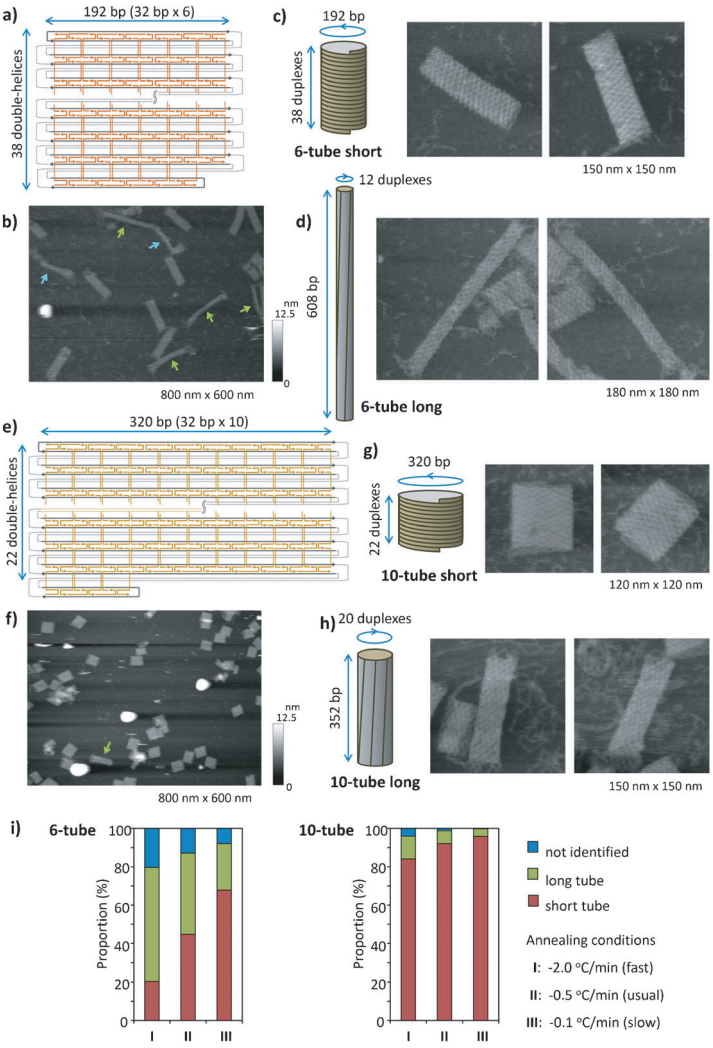

Figure 5. The 6- and 10-tube structures. a) The design of the 6-tube structure. In this design, the 38 layers of 192 bp dsDNAs are helically assembled to form a tubular structure. b) AFM image of 6-tubes after assembly. The green and blue arrows represent long tubes and long/short mixed tubes, respectively. c) AFM images of short 6-tubes. d) AFM images of long 6-tubes. e) The design of the 10-tube structure. In this design, the 22 layers of 320 bp dsDNAs are helically assembled to form a tubular structure. f) AFM image of 10-tubes after assembly. The green arrow represents a long tube. g) AFM images of short 10-tubes. h) AFM images of long 10-tubes. i) Proportion of the formation of the short and long 6-tube (left) and 10-tube (right) using different annealing conditions.

Table 3: Measurement of the dimensions (in nm) of 6- and 10-tube.[a]

	6-tube short	6-tube long	10-tube short	10-tube long
length	118.7 ± 4.5	201.5 ± 7.6	73.2 ± 4.4	119.7 ± 5.8
width	32.6 ± 2.6	13.7 ± 2.4	58.6 ± 3.4	28.1 ± 1.8

[a] Mean values ± standard deviation.

Table 4: Observed angles (in °) on the tube surface of short and long 6- and 10-tubes.[a,b]

	6-tube short		6-tube long		10-tube short		10-tube long	
Direction of M13 strand	L	R	L	R	L	R	L	R
Direction of helical axes	L	R	R	L	L	R	R	L
angle θ	28.6 ±1.9	35.2 ±2.4	40.2 ±4.7	16.3 ±2.3	30.4 ±1.6	34.6 ±2.2	38.1 ±4.3	21.9 ±3.3
angle ψ	32.8 ±0.9	27.3 ±1.6	13.5 ±2.9	43.2 ±4.7	34.6 ±2.6	28.3 ±1.7	18.0 ±2.7	38.3 ±3.5
tubes analyzed	38	6	33	6	46	19	29	8

[a] Mean values ± standard deviation. [b] L: left-handed, R: right-handed.

tubes, which were categorized to unidentified tubes. Moreover, we also observed long tubes with short tubular structures attached at the both ends (Figures 5b and S11). These incomplete products failed to isomerize to be single structures.

In the case of 10-tubes which were assembled using the same annealing conditions, short-tube formation took place with 93% yield, whereas long tubes were few (5%) (Figures 5f,i and S12). In this case, the structural stress involved in the formation of the short 10-tubes should be small because of moderate bending of the bundled dsDNAs around the tube body. The direction of the helices in the short and long tube was mainly left-handed (ca. 70%) and right-handed (ca. 80%), respectively, and opposite helical tubes were observed as minor products. The moderate curvature of the tube surface may produce short and long tubes with both helical directions. The length of short 10-tubes, which consisted of 22 layers of bundled dsDNAs, was 73 nm, so that the width of one layer was calculated to be 3.3 nm. We estimated the diameter of short 10-tubes from the width of the tube as 37 nm. This value was close to the expected diameter (35 nm) from the design, in which the diameter was roughly calculated from a circumference of 320 bp (109 nm). The length of long 10-tubes, which were composed of 352 bp of bundled dsDNAs, was 120 nm, which was the same as the expected length (120 nm). The width of long 10-tubes, which consisted of 20 bundled dsDNAs, was 28 nm, and the center-to-center distance between the adjacent helices was calculated to be 2.8 nm, so that the diameter of long 10-tubes was estimated to be 18 nm.

We prepared tubes with three different sizes, 6-, 8-, and 10-tubes, which included short and long ones. The formation of the short and long tubes depended on the diameter and annealing speed. In a series of left-handed short tubes, the angles of the surface pattern of 10-tubes were larger than those of 6- and 8-tubes, and the width of the layer of 6-tubes (3.1 nm/layer) was smaller than that of 8- and 10-tubes (3.3 nm/layer). These results indicate that the length of short 6-tubes was slightly compressed, because of resistance to the bending of bundled double helices along the helical axes. In a series of right-handed long tubes, the direction of the axis of bundled helices derived from the surface pattern of 10-tubes exhibited a smaller angle than those of 6- and 8-tubes. Furthermore, the center-to-center distance between the adjacent helices in 6-tubes (2.3 nm) was smaller than that observed in 8- and 10-tubes (2.8 nm). These results suggest that long 6-tubes have a more twisted and packed structure compared with long 8- and 10-tubes. One explanation for the preference of long-tube formation among 6-tubes is the helical stress during the formation of the structure. However, the packing of the bundled helices of long 6-tubes should be better than that of other tubes, meaning that long 6-tubes are more stable than expected.

We have developed a novel method to construct size-controlled helical tubular structures using the DNA origami method, analyzed the structures of the tubes in detail, and estimated the corresponding folding processes. Although the relationship between the chirality and design of the tubular structures is still unclear, the preferential chirality of the tubes could be simulated by molecular dynamics studies such as canDo analysis.[25] In terms of the isomerization of the Holliday junction,[22] the dynamic structural change of the tubular structures could be induced by applying the force outside; this system could be employed for creating an elastic nanomachine.

Received: March 3, 2014
Revised: April 28, 2014
Published online: May 30, 2014

Keywords: atomic force microscopy · DNA nanotechnology · DNA origami · DNA tube · isomerization

[1] N. C. Seeman, *Annu. Rev. Biochem.* **2010**, *79*, 65–87.
[2] S. M. Douglas, H. Dietz, T. Liedl, B. Hogberg, F. Graf, W. M. Shih, *Nature* **2009**, *459*, 414–418.
[3] E. S. Andersen, M. Dong, M. M. Nielsen, K. Jahn, R. Subramani, W. Mamdouh, M. M. Golas, B. Sander, H. Stark, C. L. Oliveira, J. S. Pedersen, V. Birkedal, F. Besenbacher, K. V. Gothelf, J. Kjems, *Nature* **2009**, *459*, 73–76.
[4] M. Endo, K. Hidaka, T. Kato, K. Namba, H. Sugiyama, *J. Am. Chem. Soc.* **2009**, *131*, 15570–15571.
[5] D. Han, S. Pal, Y. Liu, H. Yan, *Nat. Nanotechnol.* **2010**, *5*, 712–717.
[6] A. Kuzyk, R. Schreiber, Z. Fan, G. Pardatscher, E. M. Roller, A. Hogele, F. C. Simmel, A. O. Govorov, T. Liedl, *Nature* **2012**, *483*, 311–314.
[7] C. Lin, R. Jungmann, A. M. Leifer, C. Li, D. Levner, G. M. Church, W. M. Shih, P. Yin, *Nat. Chem.* **2012**, *4*, 832–839.
[8] J. Fu, M. Liu, Y. Liu, N. W. Woodbury, H. Yan, *J. Am. Chem. Soc.* **2012**, *134*, 5516–5519.
[9] P. W. Rothemund, A. Ekani-Nkodo, N. Papadakis, A. Kumar, D. K. Fygenson, E. Winfree, *J. Am. Chem. Soc.* **2004**, *126*, 16344–16352.
[10] J. C. Mitchell, J. R. Harris, J. Malo, J. Bath, A. J. Turberfield, *J. Am. Chem. Soc.* **2004**, *126*, 16342–16343.
[11] M. Endo, N. C. Seeman, T. Majima, *Angew. Chem.* **2005**, *117*, 6228–6231; *Angew. Chem. Int. Ed.* **2005**, *44*, 6074–6077.
[12] Y. Ke, Y. Liu, J. Zhang, H. Yan, *J. Am. Chem. Soc.* **2006**, *128*, 4414–4421.

[13] F. Mathieu, S. P. Liao, J. Kopatscht, T. Wang, C. D. Mao, N. C. Seeman, *Nano Lett.* **2005**, *5*, 661 – 665.
[14] A. Kuzuya, R. S. Wang, R. J. Sha, N. C. Seeman, *Nano Lett.* **2007**, *7*, 1757 – 1763.
[15] P. Yin, R. F. Hariadi, S. Sahu, H. M. Choi, S. H. Park, T. H. Labean, J. H. Reif, *Science* **2008**, *321*, 824 – 826.
[16] S. M. Douglas, J. J. Chou, W. M. Shih, *Proc. Natl. Acad. Sci. USA* **2007**, *104*, 6644 – 6648.
[17] H. Dietz, S. M. Douglas, W. M. Shih, *Science* **2009**, *325*, 725 – 730.
[18] D. Han, S. Pal, J. Nangreave, Z. Deng, Y. Liu, H. Yan, *Science* **2011**, *332*, 342 – 346.
[19] J. E. Heuser, *J. Mol. Biol.* **1983**, *169*, 155 – 195.
[20] S. A. McKinney, A. C. Declais, D. M. Lilley, T. Ha, *Nat. Struct. Biol.* **2003**, *10*, 93 – 97.
[21] P. W. Rothemund, *Nature* **2006**, *440*, 297 – 302.
[22] S. Hohng, R. Zhou, M. K. Nahas, J. Yu, K. Schulten, D. M. Lilley, T. Ha, *Science* **2007**, *318*, 279 – 283.
[23] J. P. Sobczak, T. G. Martin, T. Gerling, H. Dietz, *Science* **2012**, *338*, 1458 – 1461.
[24] S. Woo, P. W. Rothemund, *Nat. Chem.* **2011**, *3*, 620 – 627.
[25] D. N. Kim, F. Kilchherr, H. Dietz, M. Bathe, *Nucleic Acids Res.* **2012**, *40*, 2862 – 2868.

